Hungarian Association of Agricultural Informatics
European Federation for Information Technology in Agriculture, Food and the Environment

Journal of Agricultural Informatics. Vol. 10, No. 2
journal.magisz.org

Mathematical analysis of drone flight path

Róbert Barna[1], Kristóf Solymosi[2], Eleonóra Stettner[3]

I N F O
Received 12-11-2019
Accepted 27-12-2020
Available online 28-01-2020
Responsible Editor: M. Herdon:

Keywords:
drone, overlap, footprint, geometry, GeoGebra

A B S T R A C T

In practice, the drone may not always be able to follow a pre-planned flight path. Therefore, producing orthophotos can be problematic. The drone's shooting positions can be read from the captured images, so the actual flight path is known. The recorded route data and camera properties can be used to calculate the photographed area. It is a prerequisite for making an orthophoto that the adjacent images overlap a certain percentage. Calculating the area of an overlapping rectangle is lengthy by specifying the coordinates of the intersecting sides. We have developed a simpler method for this. One of the two overlapping rectangles was fixed and examined to determine the curve of the center of the other rectangle such that the overlapping area was exactly equal to the required overlap. This curve has become a hyperbola arc. This makes the calculation simpler and can be traced back to comparing the lengths of two sections. The method was developed using GeoGebra software.

1. Introduction

Nowadays, aerial photography and more specifically unmanned aerial vehicles (UAVs) extended with multispectral cameras (also called Unmanned Aerial Systems, UASs) are becoming more numerous and affordable each year giving access to temporal and spatial resolutions not seen before (Wendel et al., 2006). UAVs have long been used in various, but mostly in military applications in the past. However, due to the fact that the technology is becoming more available and affordable, and because they do not require high-skill piloting anymore, they are emerging in civilian fields of use. This branch of UAVs according to size categories are the smaller (< 20 kg) ones (Laliberte and Rango,). Aerial photography and videography (both casual and professional) can hardly be thought of without the use of drones (UAVs) nowadays. In agriculture, the mapping of fields is no exception to this. Furthermore, with the help of specialized software (such as DroneDeploy or DJI GS Pro) – and, of course, with the miniaturization of technology, e.g. GPS chips – consumers can tap into the opportunity of automatic vehicle guidance for precision agriculture and smart farming needs (Eisenbeiss et al. 2009). Acquired datasets are of course digital images, associated with GPS position and related flight information. Furthermore, with mentioning only a selected few, unmanned aerial imagery has been shown to be useful for mapping spatial variability within fields (Mulla, 2013), crop monitoring for site-specific application (Shanahan et al., 2008; Merotto et al. 2012; Rasmussen et al. 2016) and so on.

Modern practice shows that UAVs have the potential to monitor and assess agricultural and environmental variables (Zhang & Kovács 2012). The main caveat of this, however, is the need to capture a large number of overlapping photos that must be stitched together to produce an orthorectified image (to exclude optical and geometrical errors for the large orthoimage, also for the sake of geo-registering every image) of the desired area (Vericat et al. 2009). Important variables in

[1] Róbert Barna
Kaposvár University, Faculty of Economic Science, Institute of Methodology
barna.robert@ke.hu
[2] Kristóf Solymosi
Kaposvár University, Doctoral School in Animal Science
solymosi.kristof@ke.hu
[3] Eleonóra Stettner
Kaposvár University, Faculty of Economic Science, Institute of Methodology
stettner.eleonora@ke.hu

using drone imagery for mapping weeds are the image spatial resolution and the phenological stage of the crop being photographed (as higher the spatial resolution is, the finer the details are on the conjoined image as well) (Gómez & Candón 2014). It is clearly observable that using other types of remote platforms with coarse spatial resolutions, such as satellite imagery has huge limitations in precision practices.

It is very important to assess the accuracy of orthomosaiced images. Co-registration of them is usually expressed in RMSE and is dependent on the camera internal and external orientation (thus gimbal positions) and the density and distribution of ground control points (GCPs), plus the topographic complexity of the scene. (Vericat et al. 2009)

One of the main factors to have an adequate orthophoto is the amount of vertical and horizontal overlap. The photogrammetry is capable of producing 3D models of the joint area of 2D images if overlapped by at least 60% (Detrekői & Szabó, 2013).

The aircraft movement can be described relative to the aircraft body (body frame). Three perpendicular axes are defined such that the origin is the center of mass, and the X axis is directed through the front of the aircraft and the Y axis through the right of the aircraft, and the Z axis is finally through the bottom of the aircraft (forward, right and downward rotation respectively). When describing rotational movement, the X, Y and Z axes are renamed Roll (X), Pitch (Y) and Yaw (Z), and that is the nomenclature that we are using through the article (Figure 1).

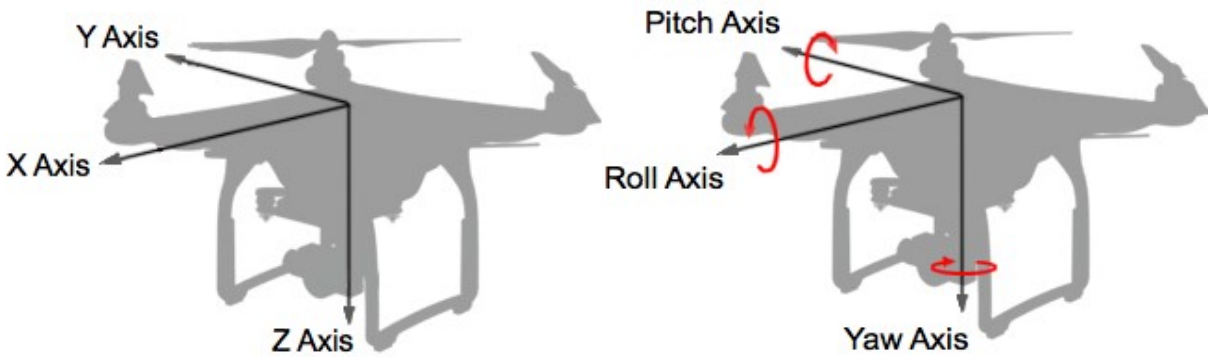


Figure 1. X,Y,Z and Roll, pitch and yaw axes on a drone
(DJI.com 2016)

The orientation of the aircraft and gimbal is known as its altitude and is defined by the rotation around the pitch, roll and yaw axes. Half of the aircraft's propellers spin clockwise, while the other half anti-clockwise. When all spin with equal speed, the aircraft heading will be constant. If one spins faster than the other, the aircraft will rotate around the yaw axis (DJI.com 2016).

1.1. Problem Definition

For surveys, drones either fly a predetermined route with a fixed exposure position (Figure 2) or freehand. The drone may not always be able to follow the planned flight path, or the required coverage may not be achieved during manual control. These may cause errors in the creation of the orthophoto and 3D terrain model. Due to the large number of in-flight shots, it takes a long time to produce an orthophoto. If the error were detected before the orthophoto was produced, it could save much time.

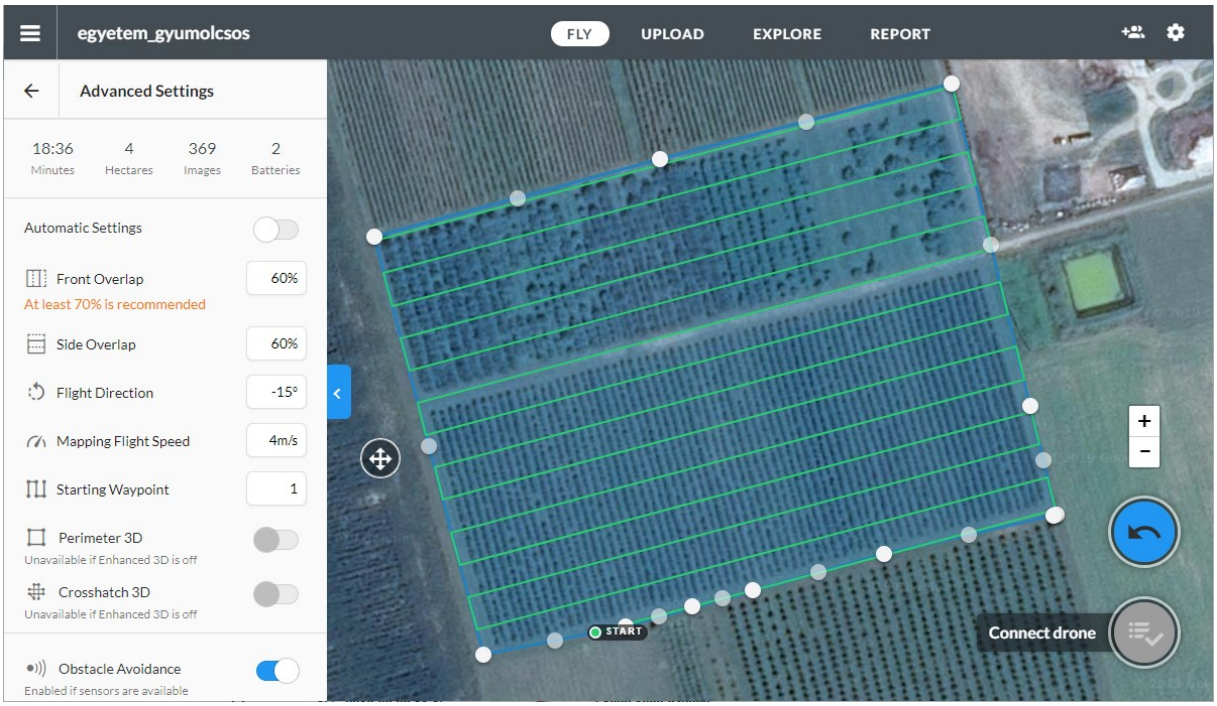


Figure 2. Flight path planned in DroneDeploy

The drone's shooting positions can be read from the captured images, so the actual flight path is known. From the recorded route data and camera characteristics, the area photographed from each drone position, the footprint, and then the coverage map of the entire flight can be calculated.

Based on this map, it can be evaluated whether the orthophoto condition is met, i.e. whether the adjacent images overlap to the required extent. To calculate the overlapping area, you first need to determine the coordinates of the intersections (*E*, *F*), and then calculate the area of the resulting overlapping rectangle (*AEGF*). If the area is known, the overlap rate can be calculated (Figure 3).

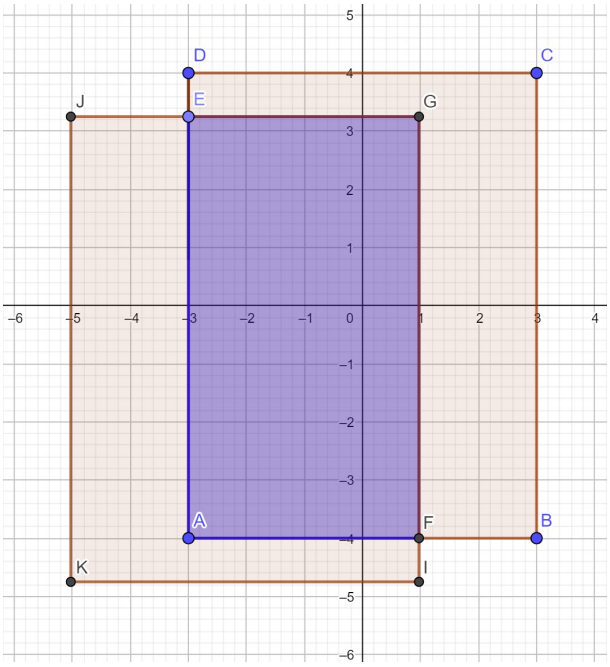


Figure 3. Footprint overlap calculation using intersection points

1.2. Goals

This calculation above can also take a long time, so we wanted to develop a fast computation algorithm that can be used to determine on the spot, after a flight, whether the captured images meet the required overlaps of the flight plan. If the result is negative, we gain the ability to retake the shots from the problematic areas immediately.

In this developed simpler method we estimate the degree of overlap based on the coordinates of the centers of the rectangles and the direction of the vector that connects them.

1.3. Disregarded factors

The effect of the relief on the footprint size was ignored during the study. We did not take into account the dimensional change due to the camera's tilt angle. During flights, the gimbal can hold the camera so well in the desired direction that the deviation from the vertical was only 0.1 degrees so far, which has a negligible effect. In flight, the rectangles of the footprints are not always parallel, but the difference is so small that we ignored it. When setting after turning, the deviation was only 1 degree and during scanning only 0.1 degrees.

2. Material and methods

GeoGebra software was used for the geometric analysis, and the calculations were made using Excel VBA programming language. We used QGIS software for mapping. We used two drones for the study, first a DJI Phantom 4 (with a modified filter on its red channel to be able to sense NIR). Main specifications are 1/2.3" CMOS, with effective pixels of 12.4 M; field of view of 84°, 20 mm (35 mm format equivalent) with f/2.8 focus at infinity; picture size of 4000×3000 pixels. The camera has a 3-axis gimbal that is capable of pitch (-90° to +30°), roll and yaw. The other drone used was a DJI Phantom 4 Pro, which has more infrared sensors (for collision avoidance) and a modified camera: 1'' CMOS with effective pixels of 20M; FOV of 84°, 8.8 mm/24 mm (35 mm format equivalent) at f/2.8, with the other main parameters being the same as the first drone mentioned.

2.1. Modeling in GeoGebra

Why did we use Geogebra for the simulation? On the one hand, Geogebra is freely accessible to anyone on every continent and is widely distributed. Geogebra.org has millions of free materials, simulations, exercises, lessons, games, and maths and other disciplines that everyone can freely browse. Another advantage of the Geogebra program is its dynamism. By changing the parameters we can observe the changes of the results. This feature of the program is heavily utilized by us. Finally, Geogebra is exceptionally applicable to finding loci (Blažek & Pech 2019, Botana & Abánades 2014).

The math problem is as follows. Given are two intersecting rectangles with parallel sides. One (*ABCD*) is fixed with center of origin, the other one is moving (*GIKJ*). Examine the set of points of the moving rectangle centers (the geometry of the centers), while the area of the resulting overlapping rectangle is constant. The sides of the original rectangles should be *2a*, *2b*, their area obviously being $A = 4ab$, the area of the overlapping rectangle should be percentage of the area of the original rectangles (in GeoGebra application $a = 3$, $b = 4$ units, $p = 60\%$). So the area of the overlapping rectangle is $4abp$.

First, *E* moves on the *DM* section. The coordinate of *M* is calculated from the consideration that *E* only makes sense to move on a given side until the sides of the fixed and moving rectangles parallel to the *x* axis overlap. So $(a - x(M) \cdot 2b = 4abp$ gives the coordinates of the point *M*: $M\ (a - 2ap, b)$. While *E* is the point of the segment *DM*, the vertex *F* of the overlapping rectangle is on the *BC* side of the fixed rectangle. Coordinates are also calculated from the $4abp$ area of the overlapping rectangle, which must give a constant value, so *F*: $F(a, b - 4abp / (a - x(E)))$. The set of *H* points can be defined by the GeoGebra GeometryLocation (<Point to Draw Geometric Location>, <Point>) command, where the first point in the command is *H* and the second is *E*.

If you also want to get the equation of the set described by *H*, you can do the following. The coordinates of $x(H) = x(E) + a$, $y(H) = y(F) + b = 2b - 4abp / (a - x(E))$, *H* will now be briefly denoted

by x and y. Express the x-coordinate $x(E)$ of both points from each of the above equations so that we get a relation between the two coordinates of the H-point, which is sorted to give the equation of the curve described by the H-point.

$$y = 2b - \frac{4abp}{2a - x}$$

This is the equation of a hyperbola, or more precisely, a piece of the hyperbola on the condition of $0 \leq x \leq 2a - 2ap$ (Figure 4).

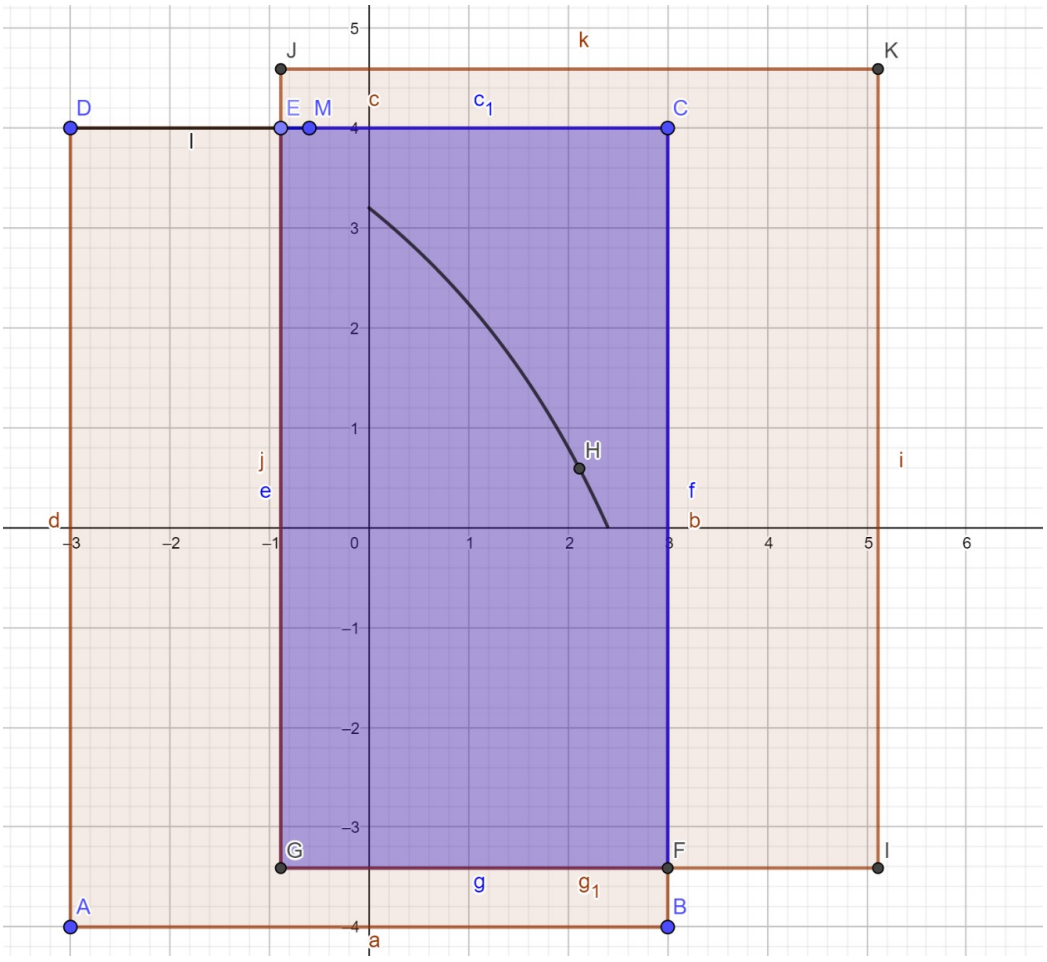


Figure 4. The hyperbola segment described by the center of the overlapping rectangle with the correct

In Figure 5, it follows from a similar idea that if E moves on the DL segment, the center of the moving rectangle H describes the equation $y = 4abp / 2a + x) - 2b$ under the condition $2ap - 2a \leq x \leq 0$.

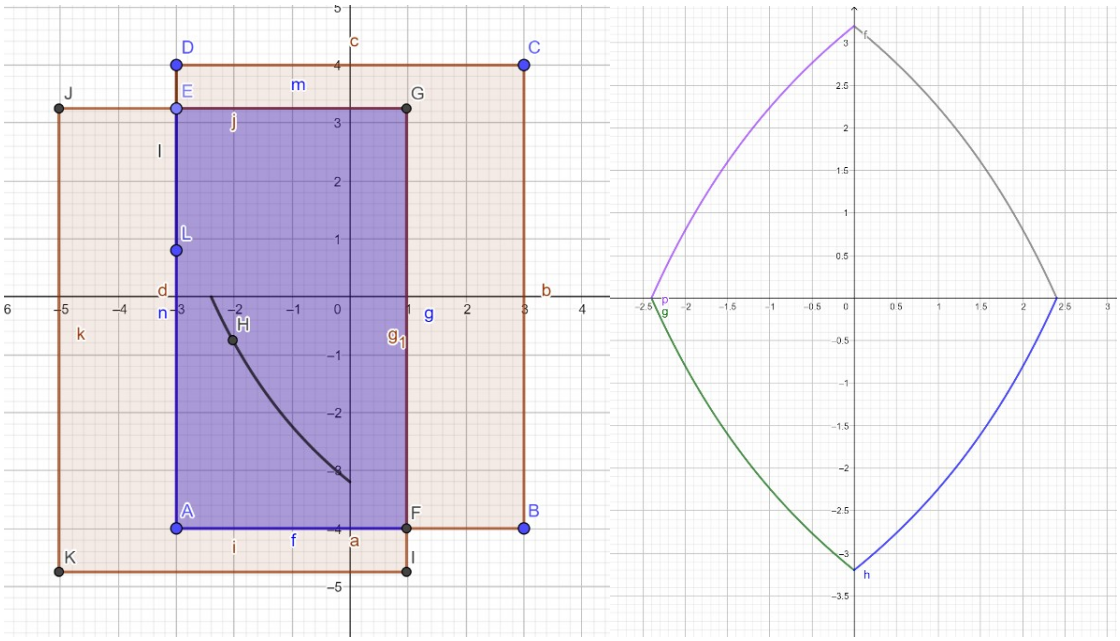


Figure 5. Hyperbola sections in the four plane quarters

For symmetry reasons, the curves shown in Figure 3 are obtained (twice each) from the point E on the other sides of the fixed rectangle to the geometric location in question.

The points of overlap required for drone flight are in the colored area in Figure 6.

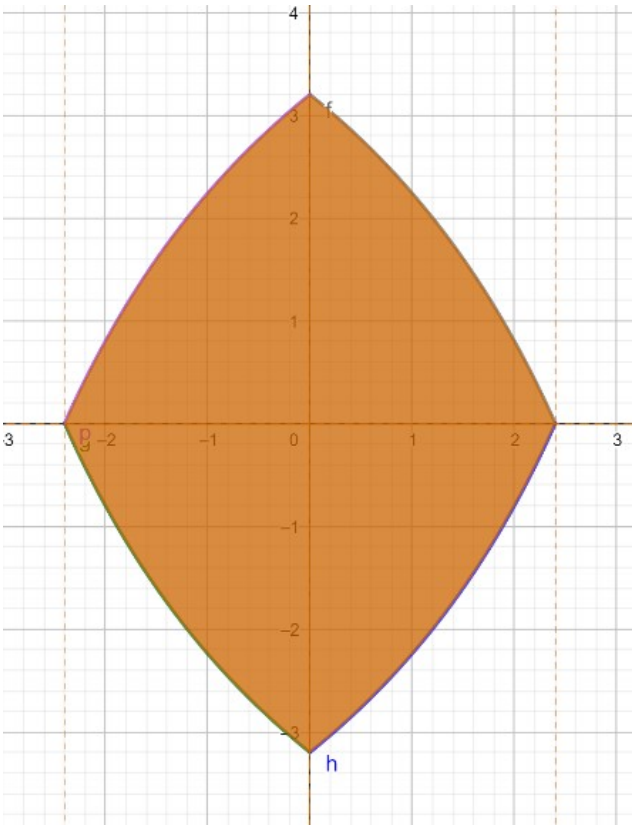


Figure 6. The area within the overlap is sufficient

The completed GeoGebra files can be consulted in the GeoGebra book on the GeoGebra website: https://www.geogebra.org/m/uksrwdw2.

2.2. The VBA program

Why did we choose the VBA programming language? Because VBA is built-in to Excel, it does not require any installation, is easy to use and provides full functionality of Excel. Because of this, it can be used to build and test the program, which, when completed, can be easily coded in a modern programming language.

Steps of the VBA program

First, we extract the EXIF data from the images into a CSV file using BR's EXIFextracter freeware software.

The image files contain EXIF (Exchangeable Image File Format) data, which holds the technical information of the images. This data is diverse, such as date and time, shutter speed, aperture, ISO, image size, GPS coordinates, and more.

Additional XMP (Extensible Metadata Platform) ISO metadata stored in the image is extracted with the VBA program. XMP includes, for example, the absolute (ellipsoidal) and relative (surface) height of the camera, the speed of the drone, the angle of the gimbal Yaw, Pitch, and Roll, etc.

The next step is that the coordinates of center of the images are converted from the WGS84 ellipsoid coordinate system used by GPS to the meter-based EOV (Uniform National Projection) coordinates used in Hungary. The calculation is based on Timár and Molnár (2002). Further calculations are also done with EOV coordinates, since this allows us to calculate in the usual Cartesian coordinate system.

To calculate the size of the photographed area, it is necessary to know the camera field of view (FOV) and the aspect ratio (aspect ratio) of the image, which can be obtained from the specification. The aspect ratio can also be calculated from EXIF data based on the image size. If the camera can capture multiple aspect ratio images, this is the better solution.

Calculating the footprint

The principle of footprint calculation is illustrated in Figure 7, and the calculation is described in detail by S. Srinivasan (2019). From the known FOV data of the drone camera and the altitude, the diameter of the footprint (DC section) can be calculated from which the known side lengths (CE and DE sections) can be calculated. Because of the center symmetry, both DE' and CE' are obtained.

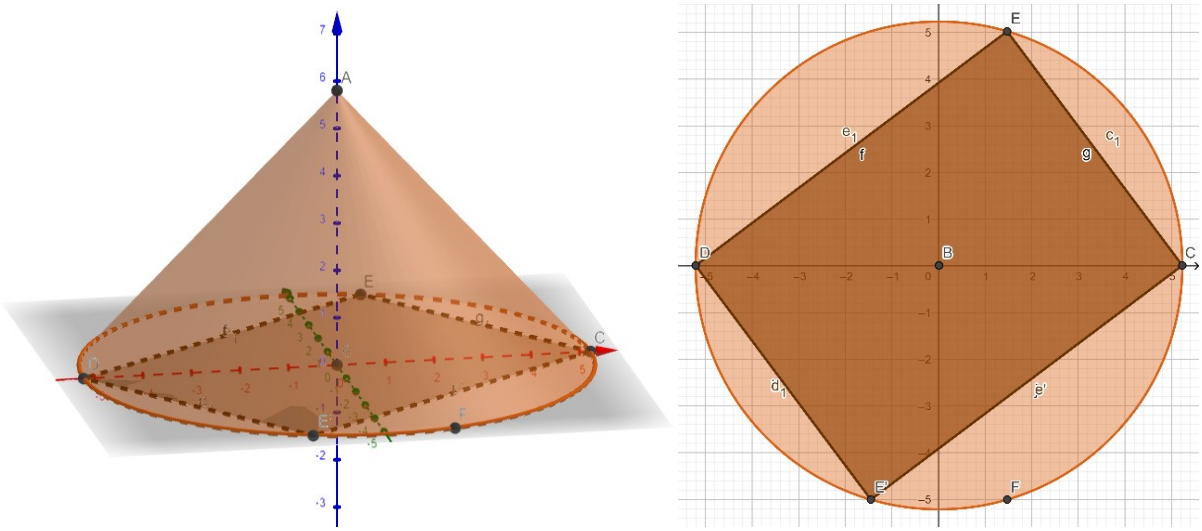


Figure 7. Principle of footprint calculation

VBA code snippet for footprint calculation based on the above:

```
Footprint_Diameter = 2 * altitude * Tan(FOV / 2 * PI / 180)
Footprint_width = Footprint_Diameter / ((1 + Picture_ratio ^ 2) ^ (1 / 2))
```

```
Footprint_height = Footprint_width * Picture_ratio
```

The rectangle (footprint) seen by the camera is rotated according to gimbal data and the coordinates of the corner points are saved.

The overlap calculation is then performed, the principle of which is shown in Figure 8. We select the rectangles in order and calculate the distance between the centers of the other rectangles (O, $O1$) with the Pythagorean theorem relative to the selected rectangle. The test is continued with rectangles having a center distance less than the shorter side length (Footprint_height).

Next, we calculate the distance (OP) between the center of the selected rectangle and the point P on the hyperbolane. The angle between the center-line segment ($\alpha + \beta$) and the shorter side of the rectangle (α) can be determined by knowing the coordinates of the corresponding points, and then calculating the angle β, which gives the equation of the line through O and P. The solution of the system of equations of the line and the hyperbola gives the coordinates of the P point. Then, using the Pythagoras theorem, we can calculate the distance of the point P of the hyperbola from the center O of the rectangle. If this is greater than the distance between the centers ($OP > OO1$), then the two rectangles overlap sufficiently.

The program counts how many other rectangles are covered to the extent needed.

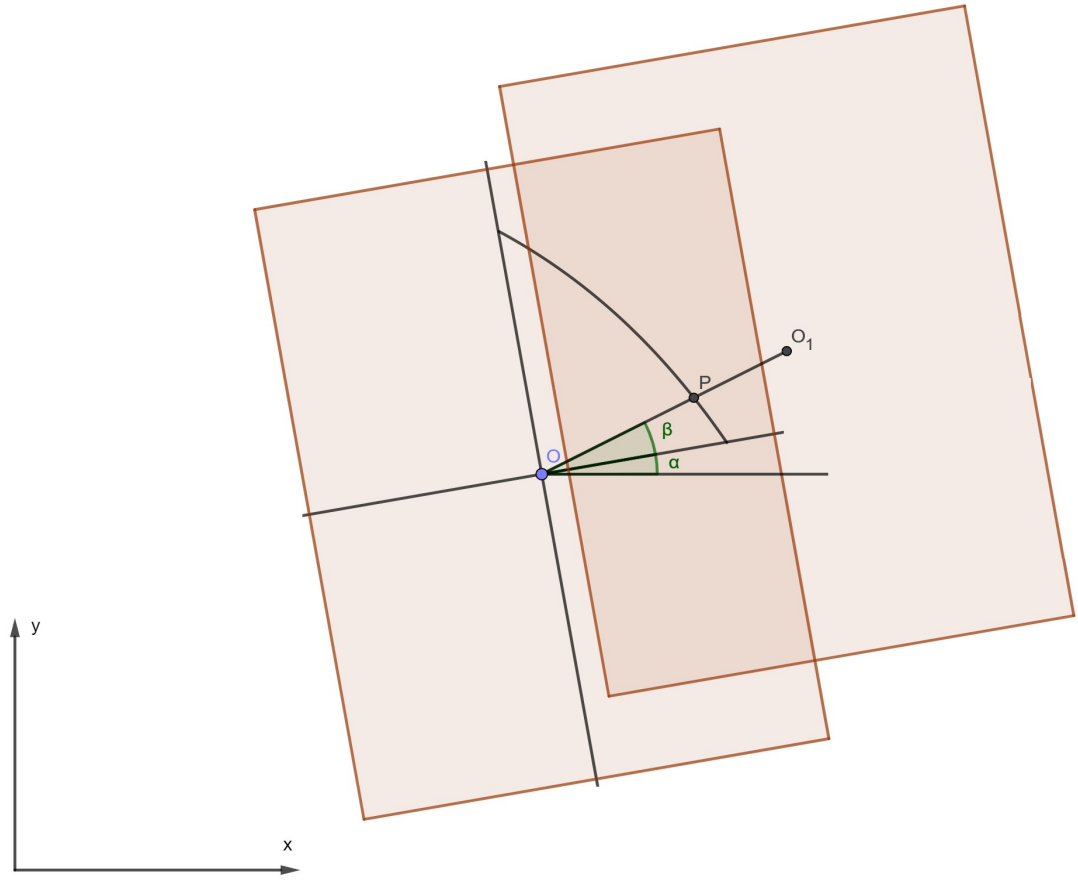


Figure 8. Scheme of overlap calculation

From the available data, the coordinates of the images, the lines connecting them, and the rectangles of the recorded areas are saved in a CSV file and plotted using QGIS.

The runtime of the VBA program depends on the number of recordings, but it produces results in hundreds of images in minutes.

3. Results

Table 1 contains the characteristics of the two flights which are illustrated.

Table 1. Attributes of the two highlighted flights

	Flight 1	Flight 2
Camera	DJI FC330	DJI FC6310
Picture size	4000x3000	4864x3648
Aspect ratio	0.75	0.75
Field of view (FOV)	84	84
Images taken	526	146
First image	DJI_0394.JPG	DJI_0240.JPG
Date	2019.03.20	2019.04.04
Time	10:51:04	11:27:39
Footprint width (m)	28.81	15.13
Footprint height (m)	21.61	11.35
Pixel size (m)	0.0072	0.0031
Front overlap	60%	60%
Side overlap	60%	60%
Relative Altitude (m)	20	10.5

First, we show the layers produced in QGIS from an adequately photographed area (Figure 9). The GPS coordinates of the recordings are indicated by circles and numbered by the flight track. The GPS points are linked by arrows to show the time course of the flight. Footprints were categorized according to the number of adjacent footprints that have a front overlap of at least 60%. As you might expect, there is the least amount of overlap at the edges, but there are at least two 60% overlapping neighbors everywhere. There is also a little overlapping footprint in the middle of Track 1, where for some unknown reason there was less footage. The large number of overlaps occurred because the drone once again flew the previously recorded area after the required battery replacement.

Even in the case of lateral overlap, the edges have the smallest matching neighbors and the most in the double-photographed area (Figure 10).

Images from the area were made into a proper orthomosaic and Digital Elevation Model (Figure 11).

Figure 12 shows the footprints of manual drone control during windy conditions. The GPS points and arrows that connect them indicate the disturbances in drone path. Because of the inappropriate condition, there are several footprints that have only two neighbors and two that have just one overlapping neighbor. The problem is that one of these is not on the edge of the track.

The orthomosaic from the images did not work as expected, and a hole was created due to lack of overlap (Figure 13).

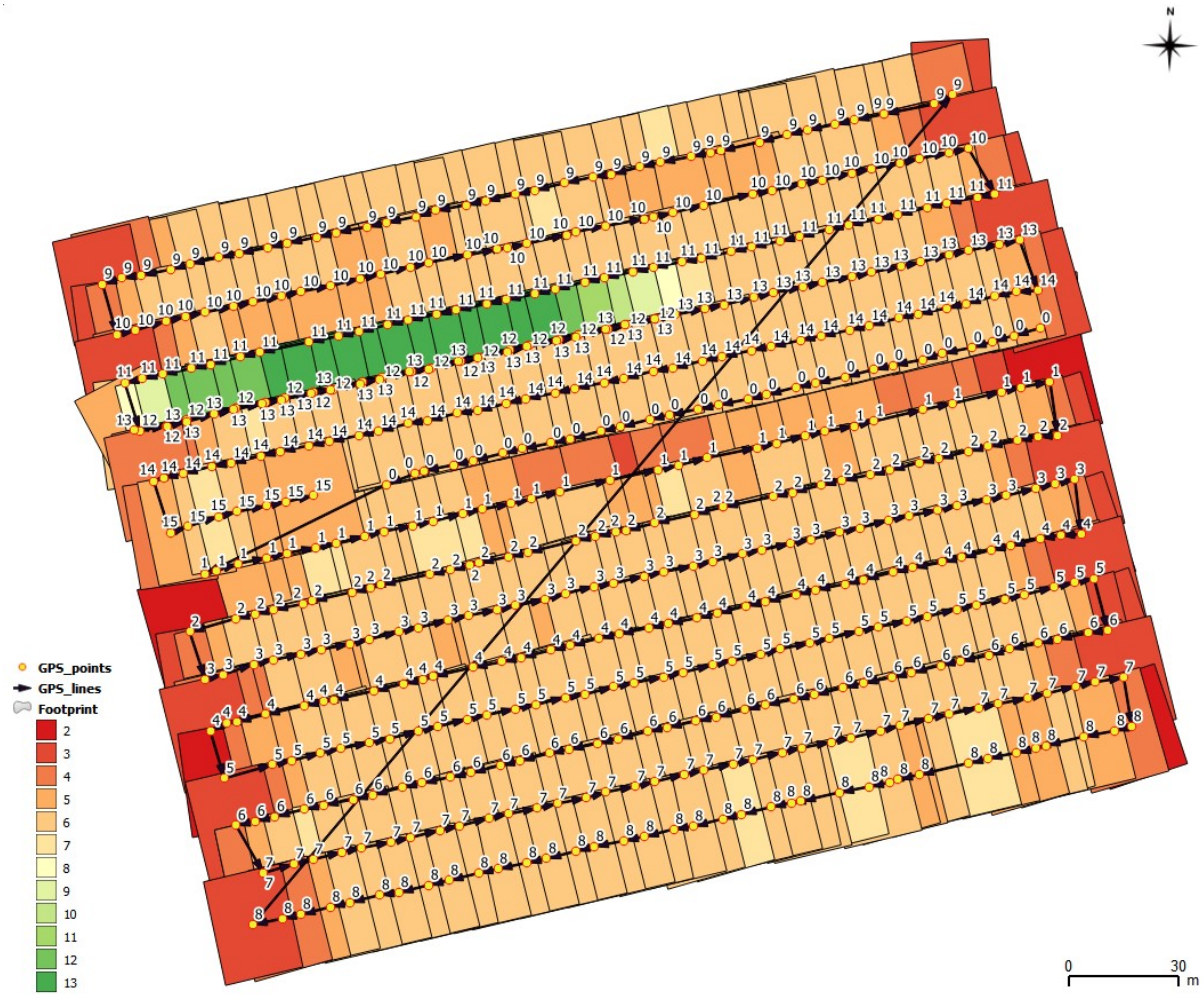


Figure 9. GPS points and lines and footprints categorized by front overlap on an adequately photographed area

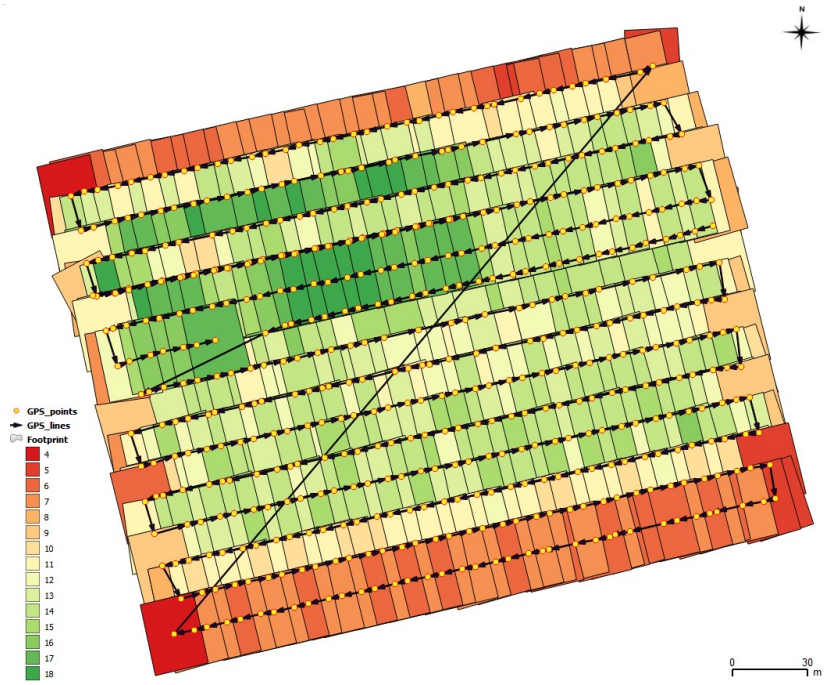


Figure 10. GPS points and lines and footprints categorized by side overlap on an adequately photographed area

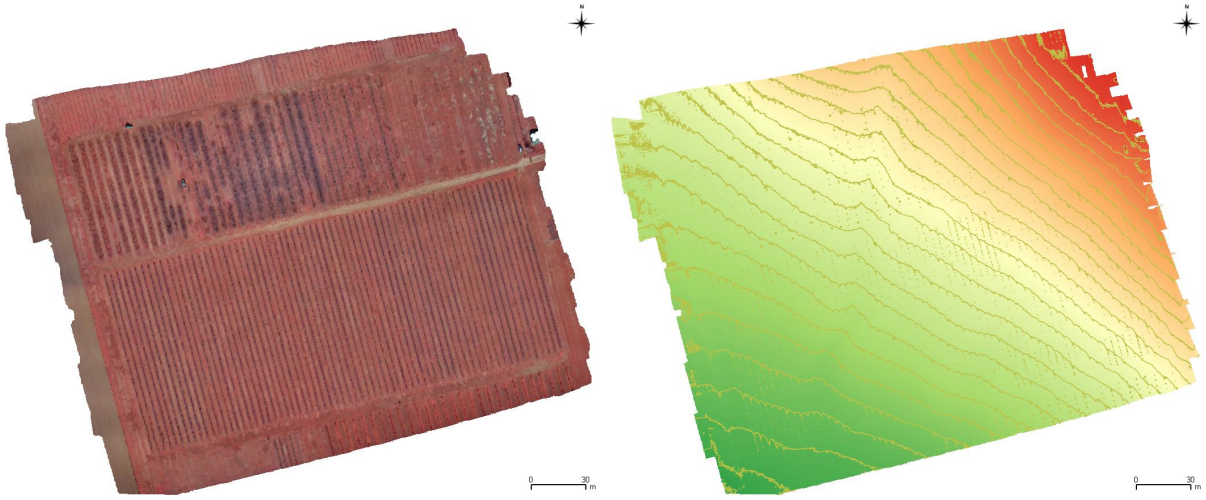


Figure 11. Orthomosaic and Digital Elevation Model from the Flight 1

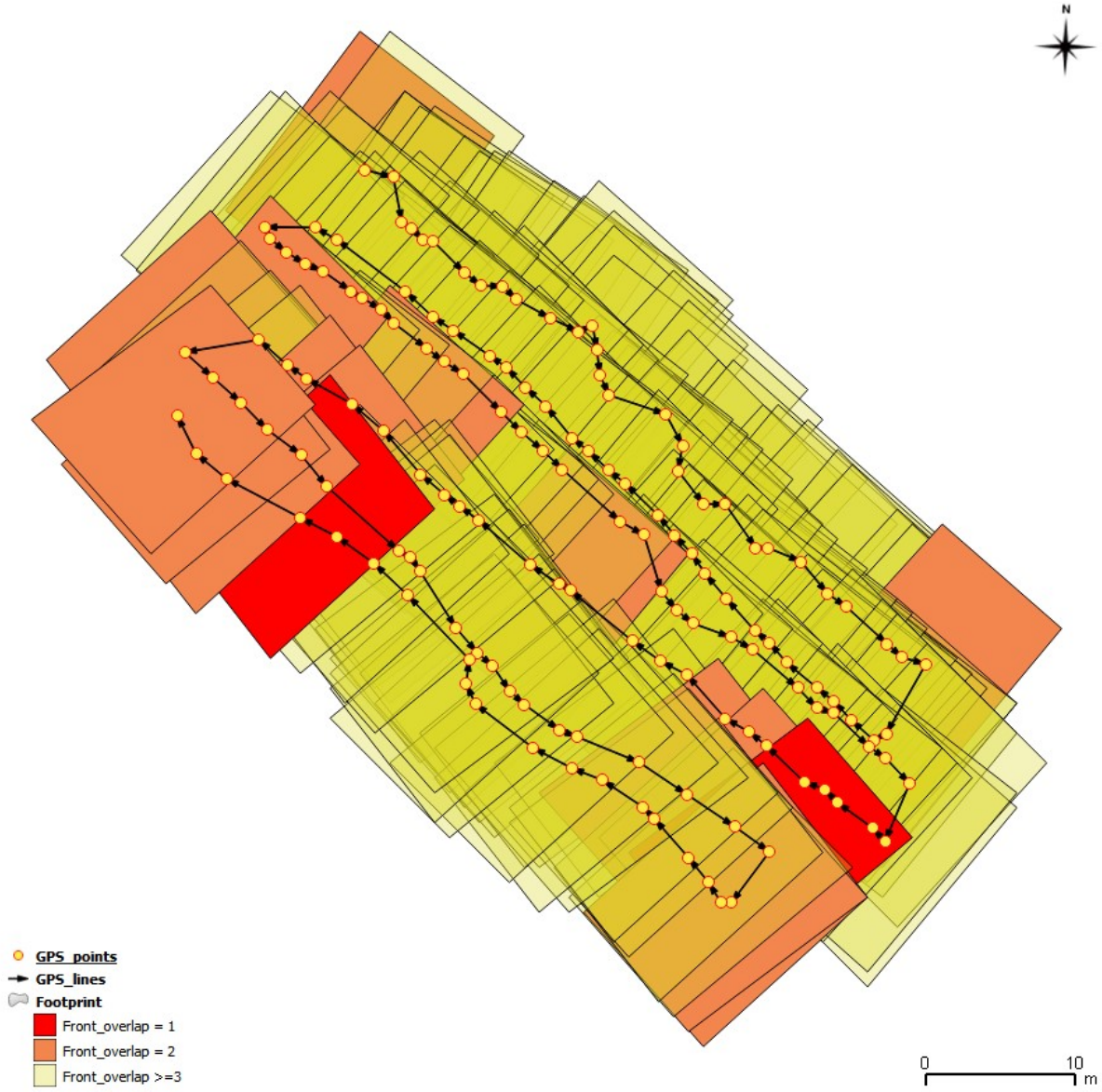


Figure 12. Footprints highlights the inadequate front overlap

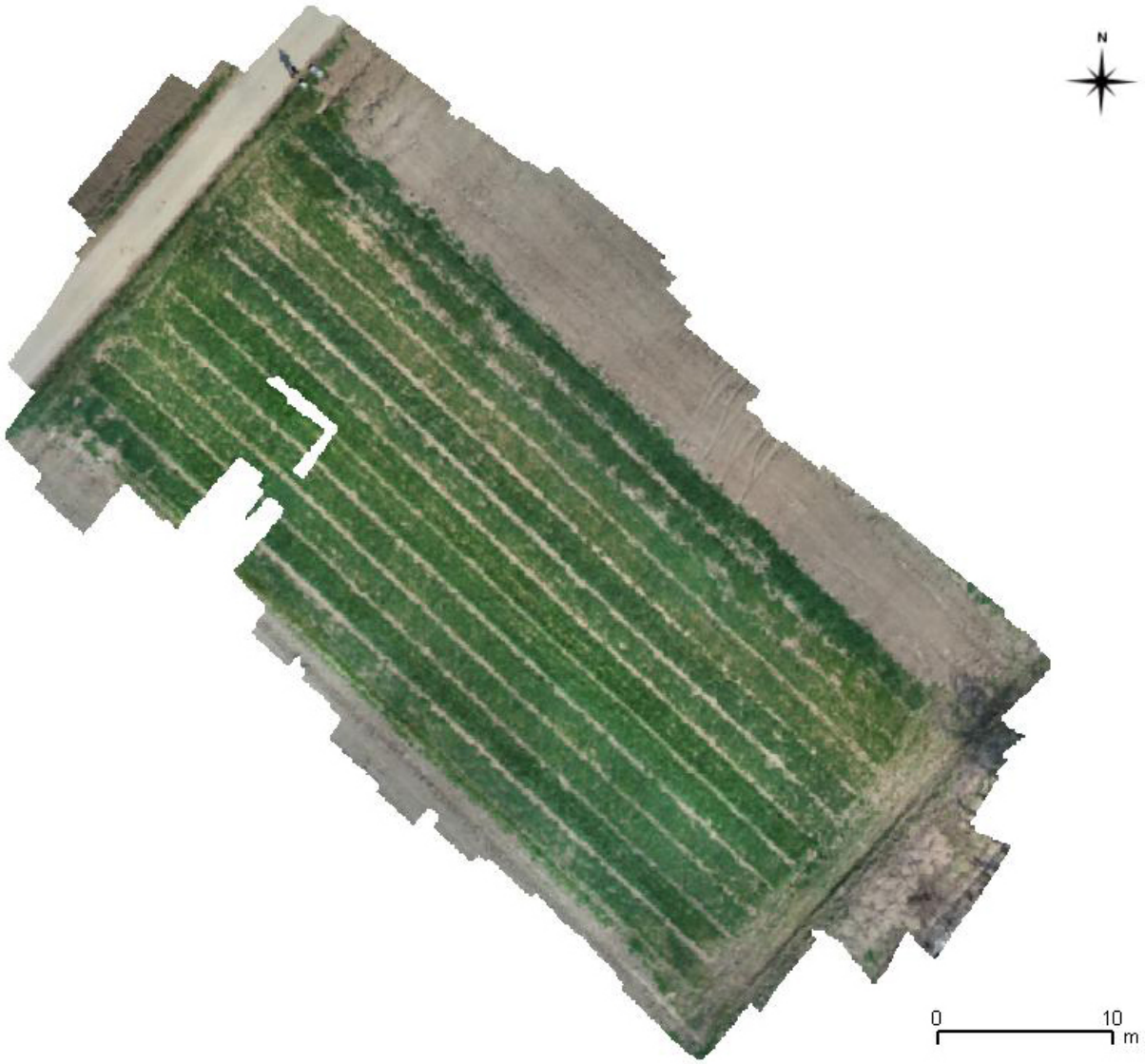


Figure 13. Orthomosaic from the Flight 2

4. Conclusions

The presented method is suitable for the examination of aerial flight recordings, even on the spot, thus allowing the re-flight of areas with poor coverage. Developed software delivers results within minutes, so it is worth considering creating a user-friendly application written in a modern programming language. Installing the application on a mobile device (smart phone, tablet) makes it easy to check for the necessary overlaps in the field.

The developed method should be checked to see if the results of the traditional geometrical methods with the usage of intersecting points (Figure 3) are different from the results outlined here. It is also worth comparing the runtime of the two versions in case of different numbers of image files.

Acknowledgements

This work is supported by the EFOP-3.6.3-VEKOP-16-2017-00008 project. The project is co-financed by the European Union and the European Social Fund.

References

Detrekői, Á. & Szabó, Gy. 2013 'Térinformatika – Elmélet és alkalmazások' Typotex Kiadó ISBN: 978-963-4930-16-7. 292. p.

Blažek, J. & Pech, P. 2019 'Locus Computation in Dynamic Geometry Environment' *Mathematics in Computer Science*, vol 13. no. 1-2. pp. 31-40. https://doi.org/10.1007/s11786-018-0355-3

Botana, F. & Abánades, M.A. 2014 'Automatic deduction in (dynamic) geometry: Loci computation' *Computational Geometry*, vol 47. no. 1. pp.75-89. doi: 10.1016/j.comgeo.2013.07.001

DJI.com 2016 'Flight Control' (Online) https://developer.dji.com/mobile-sdk/documentation/introduction/flightController_concepts.html. (Accessed: 17 June, 2019)

Eisenbeiss, H., Stempfhuber, W. & Kolb, M. 2009 'Genauigkeitsanalyse der 3D-Trajektorie von Mini-UAVs' Zukunft mit Tradition "29. Wissenschaftlich-Technische Jahrestagung der DGPF", Eds. Seyfert, E. & Deutschen Gesellschaft für Photogrammetrie, Fernerkundung und Geoinformation (DGPF) e.V., Potsdam, pp. 407-417.

Gómez-Candón, D. De Castro, A.I. & López-Granados F. 2014 'Assessing the accuracy of mosaics from unmanned aerial vehicle (UAV) imagery for precision agriculture purposes in wheat' *Precision Agric,* vol 15 pp. 44–56. doi: 10.1007/s11119-013-9335-4

Laliberte, A.S. & Rango, A. 2011. 'Image processing and classification procedures for analysis of subdecimeter imagery acquired with an unmanned aircraft over arid rangelands' *GIScience & Remote Sensing*, vol. 48. no. 1. pp. 4–23. doi: 10.2747/1548-1603.48.1.4

Merotto, A., Bredemeier, C., Vidal, R.A., Goulart, I.C.G.R., Bortoli, E.D. & Anderson, N.L. 2012 'Reflectance indices as a diagnostic tool for weed control performed by multipurpose equipment in precision agriculture' *Planta Daninha*, vol. 30. no. 2. pp. 437–447. doi: 10.1590/S0100-83582012000200024

Mulla, D.J. 2013 'Twenty five years of remote sensing in precision agriculture: Key advances and remaining knowledge gaps' *Biosystems Engineering*, vol. 114. no. 4. pp. 358–371. doi: 10.1016/j.biosystemseng.2012.08.009

Rasmussen, J., Ntakos, G., Nielsen, J., Svensgaard, J., Poulsen, R.N. & Christensen, S. 2016 'Are vegetation indices derived from consumer-grade cameras mounted on UAVs sufficiently reliable for assessing experimental plots?' *European Journal of Agronomy*, vol. 74. pp. 75–92. doi: 10.1016/j.eja.2015.11.026

Shanahan, J.F., Kitchen, N.R., Raun, W.R. & Schepers, J.S. 2008. 'Responsive in-season nitrogen management for cereals' *Computers and Electronics in Agriculture*, vol. 61. no. 1. pp. 51–62. doi: 10.1016/j.compag.2007.06.006

Srinivasan S. 2019 'Calculating a drone camera's image footprint OR How I learned to love tan again' (Online) https://www.techforwildlife.com/blog/2019/1/29/calculating-a-drone-cameras-image-footprint (Accessed: 10 June, 2019)

Timár G. & Molnár G. 2002 'A HD72 -> ETRS89 transzformáció szabványosítási problémái' *Geodézia és Kartográfia,* vol. 54. no. 12. pp. 28-30. ISSN 0016-7118

Vericat, D., Brasington, J., Wheaton, J., & Cowie, M. 2009 'Accuracy assessment of aerial photographs acquired using lighter-than-air blimps: Low-cost tools for mapping river corridors' *River Research and Applications,* vol. 25. no. 8. pp. 985-1000. doi: 10.1002/rra.1198

Wendel, J., Meister, O., Schlaile, C. & Trommer, G.F. 2006 'An integrated GPS/MEMS-IMU navigation system for an autonomous helicopter' *Aerospace Science and Technology*, vol. 10. no. 6. pp. 527-533. doi: 10.1016/j.ast.2006.04.002

Zhang, C. & Kovacs, J.M. 2012 'The application of small unmanned aerial systems for precision agriculture: A review' *Precision Agriculture* vol. 13. pp. 693–712. doi: 10.1007/s11119-012-9274-5